JTTEE5 18:896–908
DOI: 10.1007/s11666-009-9341-2
1059-9630/$19.00 © ASM International

Modeling of Combustion as well as Heat, Mass, and Momentum Transfer During Thermal Spraying by HVOF and HVSFS

Esther Dongmo, Rainer Gadow, Andreas Killinger, and Martin Wenzelburger

(Submitted February 12, 2009; in revised form April 17, 2009)

In thermal spray technologies and coating industries, increasing research and development efforts have been made in recent years toward submicron and nanostructured layers on different materials and components, promising large potentials in functional and structural coating properties. These potentials have been encouraging researchers to aim for an improved understanding and optimization of the high-velocity oxide fuel (HVOF) system to be able to improve process control, and thus, control coating properties and enable better applications for submicron and nanostructured coatings. Moreover, on the experimental side, new thermal spray technologies have been developed in order to process nanopowders, i.e., mainly suspension-based technologies like suspension plasma spraying or high-velocity suspension flame spraying (HVSFS). HVSFS is a suitable processing method for submicron and nanoscaled particles to achieve dense surface layers in supersonic mode with a refined final structure, which is the prerequisite for improved or even superior mechanical and physical properties. However, theoretical understanding of the chemical and thermodynamic phenomena occurring in the HVOF and HVSFS reacting flow field, which is necessary for process modeling, is a challenging, multidisciplinary issue. In this study, the combustion processes as well as the heat-, mass-, and momentum interactions between the flame, the suspension droplets (including vaporization), and the solid spray particles are analyzed, taking into account both the HVOF and HVSFS spray processes. The processes are modeled and numerical simulation experiments are described. Thereby, the models are giving a detailed description of the relevant set of parameters describing the complete spraying process in the combustion chamber and expansion nozzle, respectively. Simulation results can be applied for improved process control as well as torch design, e.g., adaptation of combustion chamber design to the trajectories and dwell time of spray particles for heat transfer optimization.

Keywords computational fluid dynamics, high-velocity oxygen-fuel, high-velocity suspension flame spraying, multiphase flow, numerical analysis, process modeling, propane combustion

1. Introduction

Complex specifications of technical products in today's industries and consumer markets require with increasing frequency, the application of advanced surface technologies (Ref 1, 2). Moreover, economic factors lead to increasing importance of surface technologies. Thermal spraying offers coating processes for parts with many different coating materials in order to yield wear and corrosion resistant as well to increase the service life of many components. Macroeconomics experts have estimated that tribological and corrosion damage cause important losses in all industrial fields. The direct cost of corrosion in the United States and the European Union has been estimated at 3-5% of the Gross Domestic Product of the member states (Ref 1, 3). As a consequence, surface technologies have to be considered as one of the key technological fields in manufacturing and production industries. Thereby, engineers in industry relevant research and development face three essential tasks:

- transformation of part specifications into material and surface properties,
- integration of process technologies into corresponding process chains, and
- consideration of cost targets and ecological aspects.

One of the great challenges in thermal spray technologies to date is the manufacturing of very fine or even nanostructured coatings. This development is motivated by the fact that theirs properties are superior to those of conventional metal or ceramic coating materials, including higher strength, hardness, and ductility as well as lower porosity and surface roughness in the as-sprayed condition (Ref 4, 5).

Powders composed of nanosized particles (<100 nm) are extremely critical in handling and processing. The

Esther Dongmo, Rainer Gadow, Andreas Killinger, and **Martin Wenzelburger**, Institute for Manufacturing Technologies of Ceramic Components and Composites (IMTCCC), Universität Stuttgart, Allmandring 7b, Stuttgart 70569, Germany. Contact e-mail: esther.dongmo@ifkb.uni-stuttgart.de.

potential of these materials to pose risks to health is not yet fully examined and understood. Nanoscaled particles easily distribute in air, penetrate the human skin or pass through the respiratory tract and the lung, finally entering the blood circuit. As a result, such powders cannot be processed by conventional powder feeder techniques. Not only that safety aspect forbid any refilling, cleaning, etc., under habitual conditions, but mechanical feeding is virtually impossible due to the strong particle agglomeration because of their large specific surface that prevents good flowability. In some cases, processing of fine powders with regular powder-feeder systems can be made by using agglomerated and partially sintered powders with secondary particle sizes in the micrometer range. However, agglomeration will disturb and change the initial microstructure, and thus, also lead to restrictions in the refinement of the final coating structure.

Direct processing of powders in the form of a suspension (in aqueous or organic solvent) can solve these problems. Handling of the powders is safe, and feeding of the liquid can be realized with quite simple techniques, leading to entirely new thermal spray methods such as suspension plasma spraying (SPS), solution precursor plasma spraying (SPPS), or high-velocity suspension flame spraying (HVSFS) (Ref 1, 2, 6-9).

HVSFS is based on the conventional high-velocity oxide fuel (HVOF) thermal spray process and was developed with the aim of spraying submicron or nanoparticle suspensions with hypersonic speed to deposit thin and very dense coatings (Ref 6, 10, 11). However, for a three-phase flow system (gas: combustion gases and evaporated suspension/liquid: suspension/solid: spray particles) involving chemical reactions such as the HVSFS process, the heat and mass transfer processes and interactions between the process boundary conditions are very complex, making experimental process optimization a cost and time intensive procedure. Therefore, HVSFS spray technique needs a fundamental understanding of the thermochemical, thermodynamic and transport phenomena taking place during the combustion process and energy transfer (heat, mass, and momentum) in HVOF and HVSFS systems. In this context, modeling and numerical simulation are used to analyze and visualize these processes, and thus, increase process knowledge, further development and enable process optimization for specific product applications. Moreover, detailed understanding of thermal spray processes is also necessary for their integration in complete manufacturing process chains and for improved process efficiency and cost reduction.

In this work, 3D modeling and analysis of the combustion and gas dynamic phenomena, including modeling of the solvent evaporation and analysis of the interaction mechanisms between gas and liquid as well as between gas and titania nanoparticles, are performed for an industrial TopGun®-G torch (GTV-mbH, Luckenbach, Germany). This study is aimed on the prediction of the HVSFS system's capability under various operating conditions, the determination of parameter interrelations in the process, and finally, the design of HVSFS torches should be improved based on the simulation results. The results presented here are based on earlier work on the numerical analysis of the conventional HVOF thermal spray process (Ref 12). There, a detailed numerical description of the fluid mechanics, the transport phenomena, and the flow instabilities due to high pressure gradients is given for the free jet range (spray distance between torch outlet and the substrate). However, in this paper, only the combustion chamber and expansion nozzle are considered, while the free jet range, particle deposition, and substrate (component) will not be discussed.

2. Analytical HVOF and HVSFS Process Description

The HVOF process is complex regarding description in a theoretical model, because it involves combustion, turbulence, compressible flow, multicomponent flow, multiphase interactions, subsonic/supersonic transition, material melting, droplet deformation, and solidification. The four main physico-chemical subprocesses occurring in the thermal- and flow-field of the HVOF process can be described as follows (Ref 12, 13):

I. transformation of chemical energy into thermal energy of the gas by fuel oxidation in the combustion chamber,
II. conversion of thermal energy into kinetic energy of the gas by expansion through the nozzle, including energy transfer from the gas to the particles during this expansion process,
III. free jet flow field with flow patterns strongly depending on pressure difference between nozzle outlet and atmospheric pressure, and
IV. conversion of particles' kinetic and thermal energy into viscous deformation work and surface energy during coating deposition.

With regard to the HVSFS process, the description of subprocesses is even more complex. This is mainly because a third phase, the liquid solvent, is supplementing the solid/gas two-phase flow of the HVOF process, leading to some thermophysical and thermochemical changes on the new HVSFS process compared to the HVOF process, including evaporation and combustion of the solvent, which can lead to a cooling effect in the spray torch, and different resulting particle morphologies (Ref 6, 10, 11).

High-velocity suspension flame spraying, similar to SPS, uses a liquid solvent as carrier fluid to process nanoscale materials. Thereby, the solid powder materials are dispersed in a suspension. A suspension is a heterogeneous mixture containing solid particles and a solution or solvent (Ref 6, 9, 11). In case of the HVSFS technique, aqueous and organic solvents (water, ethanol, or isopropanol) are applied. Homogeneous dispersion of the particles can be achieved by addition of appropriate dispersing agents, while suspension stability is achieved with stabilizer additives (e.g., citric acid, acetic acid). Solid contents of suspensions for thermal spraying are in-between 10 and 15 wt.%. Subsequently, the suspensions

Table 1 Dimensionless numbers needed for process description with resp. formulae and parameters

Dimensionless quantity	Formulation		Parameters	
Damköhler number	$\mathrm{Da} = \frac{t_t}{t_c}$	(Eq 1)	t_t	Turbulent timescale
			T_c	Chemical timescale
Mach number	$\mathrm{Ma} = \frac{v_f}{u}$	(Eq 2)	v_f	Velocity of the fluid
			u	Relative sound velocity
Lewis number	$\mathrm{Le} = \frac{\lambda}{D c_p \rho}$	(Eq 3)	λ	Thermal conductivity
			D	Diffusion coefficient
			c_p	Specific heat capacity (isobar)
			ρ	Flow density
Nusselt number	$\mathrm{Nu} = f(\mathrm{Re}, \mathrm{Pr}, \mathrm{geometry}, \ldots)$	(Eq 4)		
Reynolds number	$\mathrm{Re} = \frac{\rho \cdot v d}{\mu}$	(Eq 5)	v	Fluid velocity
			d	Characteristic length
			μ	Dynamic viscosity of the fluid
			ρ	Fluid density
Prandtl number	$\mathrm{Pr} = \frac{c_p \cdot \mu}{k}$	(Eq 6)	c_p	Specific heat capacity (isobar)
			μ	Dynamic viscosity of the fluid
			k	Thermal conductivity
Weber number	$\mathrm{We} = \frac{\rho \cdot v_{rel}^2 d}{\sigma}$	(Eq 7)	ρ	Fluid density
			v_{rel}	Relative velocity fluid-droplet
			d	Droplet diameter
			σ	Surface tension of the droplet
Knudsen number	$\mathrm{Kn} \equiv \frac{\lambda}{L}$;	(Eq 8)	λ	Mean free path of molecules
			L	Characteristic dimension
	$\mathrm{Kn} = \frac{\mathrm{Ma}}{\mathrm{Re}} \sqrt{\frac{\pi \gamma}{2}}$	(Eq 9)	γ	Ratio of specific heats
Biot number	$\mathrm{Bi} = \frac{h d_p}{k}$	(Eq 10)	h	heat transfer coefficient
			d_p	Particle diameter
			k	Thermal conductivity of particles
Sherwood number	$\mathrm{Sh} = \frac{kL}{D}$	(Eq 11)	k	Mass transfer coefficient
			L	Characteristic dimension
			D	Diffusion coefficient

are ground using an attrition mill to avoid agglomerates (Ref 10, 11).

In HVSFS, the suspension is injected directly (centered and in axial direction) into the combustion chamber of the torch, where the liquid solvent is contributing to the reaction enthalpy of the combustion process (Ref 10, 11, 14). The suspension has to be fed against the combustion chamber pressure, just like in HVOF powder feeding, but with a special feeder system consisting of a pressure vessel (maximum load 10^5 Pa), in which the suspension is kept at constant pressure, and a stirring device. The injection process shows an increased complexity compared to conventional powder feeding in terms of pressure distribution and also the possibility of composition variations and *in situ* change of the composition. Therefore, an optimization of the injection behavior of suspensions was done in earlier work by modification of the nozzle geometry (Ref 6, 11, 14).

Regarding the thermophysical and thermochemical subprocesses of the HVSFS process in the combustion chamber, the following phenomena have to be considered:

I. Combustion of the fuel gas, based on the HVOF process (premixed combustion),
II. Heat, mass, and momentum transfer between the flame and the suspension droplets (organic solvent and particles), and
III. Evaporation and combustion of the suspension organic solvent (nonpremixed combustion).
IV. Agglomeration of particles and heat as well as impulse transfer from combustion gases to particles (*will not be considered in this paper*).

The chemical, thermal, thermophysical, and morphological conditions of the suspension and the particles during the process ultimately determine the coating microstructure and its macroscopic properties. Parameters such as droplet size, injection velocity, the location of solution evaporation and initial combustion, flame temperature and velocity fields in the combustion chamber and expansion nozzle can all have significant influence on the final coating structure and properties (Ref 10, 13, 15).

2.1 HVOF and HVSFS Fundamentals—Dimensionless Numbers

A detailed understanding of the basic transport phenomena as well as chemical, thermodynamic, and thermophysical phenomena are fundamental for the description and the modeling of HVOF and HVSFS processes. For example, combustion processes are based on several factors, including time and spatial dependence, the mixing condition of initial reactants, initial phases of reactants, flow conditions, rate of reaction, type of convection or diffusion, degree of compressibility of the flow, and speed of the combustion wave. Due to the complexity of these processes, some common assumptions or dimensionless numbers will be described in the following which are

relevant for modeling of the combustion, the heat and mass transfer processes as well as the type of fluid flow (Ref 1, 2, 15-17). An overview about these dimensionless numbers and the respective equations are given in Table 1.

2.2 Premixed Combustion of Propane with Oxygen

The quantitative treatment of combustion processes requires some understanding of fundamental concepts and definitions, which will be described in this section for the case of the HVOF process, using propane as fuel gas. In combustion processes, two phenomena are of increased importance:

- mixing of the reactants (fuel and oxidizer, i.e., oxygen or air) and
- the velocity of the chemical reaction (combustion) itself.

With respect to mixing of the reactants and the flow type, the HVOF combustion systems with propane as fuel gas can be characterized as a turbulent premixed flame. Fuel and oxygen are premixed in the mixing chamber before being injected into the combustion chamber at relatively high pressure (0.3-0.5 MPa). In the combustion chamber, the flame fronts propagate into a turbulent fluid flow of the exhaust gases (Ref 12-14).

The basic law of combustion of hydrocarbon materials (forward reaction), with respect to the ideal gas and chemical thermodynamic laws, is described in general case by the following chemical reactions equation whose in turn also depending on the rate coefficient k of the reaction (Ref 16, 17):

$$\text{fuel} + \text{oxidizer} \xrightarrow{k} \text{products} + \text{energy}$$
$$a\mathrm{C}_x\mathrm{H}_y + b\mathrm{O}_2 \xrightarrow{k} m\mathrm{CO}_2 + n\mathrm{H}_2\mathrm{O} + \text{energy} \quad \text{(Eq 12)}$$

Assuming that consumption or chemical reactions of the hydrocarbon species are strongly dependent on temperature and time, the reaction rate can be expressed according to:

$$\frac{d[\text{products}]}{dt} = -k \cdot [\text{reactants}]^{\text{reaction orders}} \quad \text{(Eq 13)}$$

The combustion of propane in a stoichiometric mixture (complete burning) leads to the following reaction equation:

$$\mathrm{C_3H_8} + 5\mathrm{O_2} \xrightarrow{k} 3\mathrm{CO_2} + 4\mathrm{H_2O} + 2260\ \mathrm{kJ} \quad \text{(Eq 14)}$$

The reaction rate for propane combustion is a relation between the rate coefficient and the concentration of different reactants (propane and oxygen):

$$\frac{d[\mathrm{CO_2} + \mathrm{H_2O}]}{d\mathrm{t}} = -k \cdot [\mathrm{C_3H_8}]^1[\mathrm{O_2}]^5 \quad \text{(Eq 15)}$$

According to Arrhenius (Ref 16, 17), the rate coefficient k of a combustion process depends strongly in a nonlinear way on the temperature and can be described by Arrhenius' law:

$$k = AT^b \cdot \exp\left(-\frac{E_a}{RT}\right) \quad \text{(Eq 16)}$$

where A is the pre-exponential factor ($A = 12 \times 10^{12}$ for propane oxidation), T is the local temperature with the dimensionless temperature exponent b ($b = 0$ for propane oxidation), E_a is the activation energy, and R is the universal gas constant ($R = 8.314$ J mol^{-1} K^{-1}).

Usually, the Eddy dissipation model with a stoichiometry derived from an instantaneous equilibrium code is employed to model turbulent combustion process (Ref 16). An additional (commonly used) assumption is made, saying that the chemical reaction rate is much faster than the time-scale associated with the gas dynamics according to the Damköhler number (Eq 1). The eddy dissipation model is a concept of reaction control applying in many combustion problems where reaction rates are fast compared to reactant mixing rates. The eddy dissipation model is also based on the concept that chemical reaction is fast relative to the transport processes in the flow. When reactants mix at the molecular level, they instantaneously form products. The model assumes that the reaction rate may be related directly to the time required to mix reactants at the molecular level. In turbulent premixed flows, this mixing time is dominated by the eddy properties and, therefore, the rate is proportional to a mixing time defined by the turbulent kinetic energy, and dissipation (Ref 16). In conclusion, the Eddy dissipation model assumes infinitely fast reactions and reaction rates limited by the turbulent mixing rate of fuel and oxidant.

2.3 Droplet Formation, Evaporation, and Combustion of Ethanol Solvent

The HVSFS system is characterized by a two-step combustion process. The premixed combustion of propane and oxygen is run with an excess of oxygen (lean-burn combustion), leading to excess oxygen after propane combustion which is consumed during combustion of the gaseous ethanol in a diffusion flame reaction after the evaporation of ethanol (which is injected as a liquid, carrying the spray particles) in the combustion chamber (Ref 16).

Experimental studies showed a jet stream, or open jet formation, of the suspension (in this case ethanol solution containing nanoparticles) for injection in a TopGun-G® combustion chamber at high pressure (0.3-0.4 MPa) with an injection nozzle of <1 mm in diameter, see Fig. 1. Open jet formation means that the fluid is injected as a coherent stream into the surrounding medium (combustion chamber with high pressure), while e.g., for automotive injection systems, a spray injection is applied with a diverging jet of atomized fluid. The same spray characteristics are used in the SPS system (Ref 9, 15). However, in case of the HVSFS injection, the suspension jet breaks up only downstream under the influence of fluid dynamic forces. By calculation of the suspension jet's Weber number (Eq 7), it can be evaluated if break up takes place under the injection conditions and which breakup model is appropriate for modeling of breakup and droplet

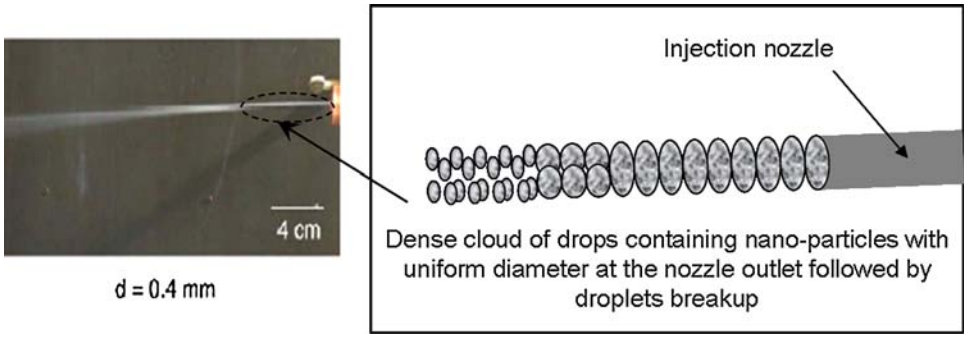

Fig. 1 Suspension droplets emerging from the injection nozzle as flow jet by HVSFS system

formation (Ref 18). The description of droplet breakup and atomization in the HVSFS system is given elsewhere (Ref 13).

Following jet and droplet breakup after injection, and thus, suspension atomization, heat transfer from the fuel gas/oxygen flame leads to vaporization of the ethanol suspension. For calculation of the interphase mass transfer liquid to gaseous ethanol by vaporization, two different correlations may be applied, depending on the specific droplet temperature and the boiling point of ethanol at the resp. pressure. The estimation of the system state can be made by applying the Antoine equation (Ref 14, 18, 19), which is given by:

$$P_{vap} = P \exp\left(A - \frac{B}{T + C}\right) \quad \text{(Eq 17)}$$

where A, B, and C are user-supplied coefficients in correlation to the solution and T is the temperature. The ethanol droplet is boiling if the vapor pressure, P_{vap}, is greater than the pressure of the gas phase, P.

Under the assumption that the ethanol temperature is above its boiling point, the mass transfer from liquid ethanol to gaseous ethanol is determined by the convective heat transfer, Q_c:

$$\frac{dm_p}{dt} = -\frac{Q_c}{V} \quad \text{(Eq 18)}$$

where m_p is the mass of the ethanol droplet and V is the temperature dependent latent heat of ethanol vaporization. If the ethanol temperature in the combustion chamber is below its boiling point, the mass transfer is given by:

$$\frac{dm_p}{dt} = \pi d \cdot D \cdot \mathrm{Sh} \cdot \frac{W_v}{W_f} \log\left(\frac{1 - X}{1 - X_f}\right) \quad \text{(Eq 19)}$$

where Sh is the Sherwood number related in Eq 11, W_v and W_f are the molecular weights of the solution vapor and the surrounded fluid, while X and X_f are the molar fractions in the drop (liquid ethanol) and in the gas phase (fuel/oxygen flame and gaseous ethanol). In either case, the rate of mass transfer is set to zero when all of the liquid substances in the particle have evaporated.

After evaporation, the gaseous ethanol undergoes a chemical reaction with the excess oxygen that remains after complete propane oxidation. The combustion of the gaseous ethanol (C_2H_6O) assuming a stoichiometric mixture (complete burning) leads to the following reaction equation:

$$C_2H_6O + 3O_2 \xrightarrow{k} 2CO_2 + 3H_2O + 1760\ \mathrm{kJ} \quad \text{(Eq 20)}$$

This combustion reaction can be described as a nonpremixed combustion, because the ethanol gas has to mix with oxygen due to molecular transport (diffusion) prior to reaction. The time needed for ethanol and oxygen to mix can be calculated from Einstein's equation for the depth of intrusion by diffusion. Additionally, calculation of the Lewis number (Eq 3) can yield information about the chemistry rate of the reaction. In case of infinitely fast ($Le \ll 1$) chemistry, the reaction of ethanol with oxygen can be approximated by a fast one-step reaction (Eq 20).

2.4 The Three Dimensional Reacting Flow Conservation Equations

For chemical reacting flows, the system is completely described by specification of pressure, density, temperature, velocity of the flow, and concentration of each chemical species as a function of the spatial coordinates and the time, respectively. A change in these parameters can result from fluid flow convection, chemical reaction, molecular transport (heat conduction, diffusion, and viscosity), or radiation (Ref 16, 17). Some properties in reacting flows are conserved, such as total energy, mass, and momentum of the flow, leading to the conservation equations (Ref 12-14, 16). At the same time, the three main thermodynamic laws (conservation of energies, irreversible process, and temperature dependence of entropy) allow the determination of the equilibrium state of a chemical reaction as well as its molecular description. Together, these correlations and laws are used for the mathematical description of chemical reacting flows.

In computational analysis, heat is calculated from temperature and velocity, work is calculated from pressure and density, and the reaction gases are calculated from concentrations of the reactants and velocities. The

governing equations of these basic values are derived from fundamental thermodynamic, hydrodynamic, and chemistry principles on a fixed mass basis or a control volume basis (Ref 16).

The process model used in this paper is based on the one-way coupling assumption. That means, the existence of particles has a negligible influence on the gas while the particle in-flight behavior depends on the thermal and flow field of the gas. This assumption is reasonable, because particle loading in the HVOF process is typically less than 5 vol.% (Ref. 12, 13).

The conservative form of the 3D Navier-Stokes equations in Cartesian coordinates describing the HVOF spray process flow field using in a transient model are as follows:

– the continuity conservation equation

$$\frac{\partial \rho}{\partial t} = -\frac{\partial \rho u_k}{\partial x_k} \quad \text{(Eq 21)}$$

– the momentum conservation equation

$$\rho \frac{\partial u_i}{\partial t} = -\rho u_k \frac{\partial u_i}{\partial x_k} - \frac{\partial p}{\partial x_i} + \frac{\partial \tau_{ik}}{\partial x_k} \quad \text{(Eq 22)}$$

– the energy conservation equation

$$\rho \frac{\partial h}{\partial t} = -\rho u_k \frac{\partial h}{\partial x_k} + \frac{\partial p}{\partial t} + u_k \frac{\partial p}{\partial x_k} + \frac{\partial}{\partial x_k}\left(\rho D \frac{\partial h}{\partial x_k}\right) + \Phi_D \quad \text{(Eq 23)}$$

and the mass conservation equation of the expanding gases (species)

$$\rho \frac{\partial Y_\alpha}{\partial t} = -\rho u_k \frac{\partial Y_\alpha}{\partial x_k} + \frac{\partial}{\partial x_k}\left(\rho D \frac{\partial Y_\alpha}{\partial x_k}\right) + S_\alpha, \quad \alpha = 1, \ldots, N_{sp} - 1, \quad \text{(Eq 24)}$$

where ρ is the density of the gas, p is the pressure, u_i is the velocity in x_i coordinate, Y_α is the mass fraction of the species and of its chemical source term S_α. Due to the scaling $\sum_\alpha Y_\alpha = 1$, $N_{sp} - 1$ species conservation equations have to be solved. The diffusion coefficient D is assumed to be equal for all components, resulting in a unity (Le = 1) Lewis number (Eq 3). This assumption is employed in order to make the reactive flow process easier to handle.

2.5 Heat, Mass, and Momentum Transport

Particulates are tracked in the continuum in a Lagrangian approach. The total forces $\sum F_i$ affecting the particle acceleration, a_p, are due to the difference in velocity between particle and fluid and due to the displacement of the fluid by the particles. The equation of motion for particles in the gas flow field is governed by Newton's law, which can be written as $m_p a_p = \sum F_i$. Thereby, the major force acting on a particle during HVOF/HVSFS spraying is assumed to be the drag force. Other forces can be neglected (Ref 12-14). Therefore, the equation of particle motion for this process has the following form:

$$m_p \frac{dV_p}{dt} = F_D \quad \text{(Eq 25)}$$

where F_D is the drag force. The drag force can be expressed as follows:

$$F_D = \frac{1}{2}\rho_g C_D A_g |U_s| U_s \quad \text{(Eq 26)}$$

The drag coefficient, C_D, is based on the Schiller-Naumann drag model and depends on the Reynolds number. For the HVOF process considered in this work, $Re > 2 \times 10^5$ according to the turbulent flow in the TopGun-G® combustion chamber. The drag coefficient C_D is calculated as follows:

$$C_D = \frac{24}{Re}(1 + 0.15 Re^{0.687}) \quad \text{(Eq 27)}$$

Particle melting or vaporization is due to heat transfer from gas to particles. This transfer is governed by three physical processes: convective heat transfer, latent heat transfer associated with mass transfer, and heat transfer by radiation. As a consequence, the equation describing the rate of temperature change for a specific particle is:

$$\sum (m_p c_p) \frac{dT_p}{dt} = Q_C + Q_M + Q_r \quad \text{(Eq 28)}$$

where T_p is the temperature of the particle and c_p is the specific heat of the particle. The convective heat transfer Q_c is calculated as:

$$Q_c = \pi d \lambda Nu (T_g - T_p) \quad \text{(Eq 29)}$$

where λ is the thermal conductivity of the gas, T_g is the temperatures of the fluid, T_p is the particle temperature, and d is the particle diameter. The Nusselt number Nu for the fluid process at hand is calculated as follows (Ref 16):

$$Nu = 2 + 0.6 Re^{0.5} \left(\mu \frac{C_p}{\lambda}\right)^{1/3} \quad \text{(Eq 30)}$$

with μ being the dynamic viscosity of the fluid. The heat transfer associated with mass transfer Q_M is given by the following relation:

$$Q_M = \sum \frac{dm_c}{dt} V \quad \text{(Eq 31)}$$

Q_M is the total amount of all components for which mass transfer is taking place and depends on the latent heat of vaporization or condensation, V. The latent heat of vaporization is a temperature dependent material property. The heat transfer by radiation Q_r is given by:

$$Q_r = \frac{1}{4}\varepsilon_p \pi d_p^2 (I - \sigma n T_p^4) \quad \text{(Eq 32)}$$

where ε_p is the emissivity of the titania particle, I is the irradiation flux on the particle surface, n is the refractive index of the surrounding gas at the location of the particle, and σ is the Stefan-Boltzmann constant.

The Biot number (Eq 10) of the ceramic particles (ratio of heat transfer coefficient on the surface to the internal heat conductivity) is assumed after analytical calculation

to be in the region of Bi < 0.1 (Ref 12). This is a suitable approximation for good heat conducting materials, for which the particles are heated with negligible internal resistance and the temperature gradients inside the particles can be ignored.

During the HVOF and HVSFS processes, cooling water surrounding the combustion chamber and the expansion nozzle leads to convective heat transfer at the wall, Q_{CWall}, of the combustion chamber and the expansion nozzle. This convective heat transfer is given by the following formulation:

$$Q_{CWall} = \pi d_{channel} \lambda_f Nu (T_f - T_{wall}) \quad \text{(Eq 33)}$$

The Nusselt number for the calculation of this heat transfer phenomenon is derived from empirical formulations for Prandtl-Taylor analogy. For a Reynolds number in the region of Re > 2300 (turbulent for pipe flow) and Prandtl number in the region of $1 <$ Pr < 50, the Nusselt number is calculated as:

$$Nu = \frac{0.04 \cdot \mathrm{Re}^{0.75}\,\mathrm{Pr}}{1 + 0.75(\mathrm{Pr}^{0.67} - 1)} \quad \text{(Eq 34)}$$

3. Modeling for Numerical Analysis

3.1 Geometrical Design

The geometrical design applied in this work for modeling of the HVOF and HVSFS process is based on the TopGun®-G torch from GTV-mbH, Luckenbach, Germany. The torch consists of a combustion chamber and a convergent-straight expansion nozzle. The fuel gas (here: propane) and oxygen are separately injected through various small channels into a mixing chamber before entering the combustion chamber as a premixed oxy/fuel mixture.

The major difference between the HVOF and HVSFS processes is the preparation and processing of the coating material. Powder materials (HVOF) or suspension droplets (HVSFS) are directly axially injected into the combustion chamber of the torch, where the oxy/fuel mixture is burned (HVOF and HVSFS) and the solution is evaporated and burned (HVSFS). The spray particles are molten and accelerated by the expanding gas jet onto the substrate surface. The computational domain of the two components, combustion chamber and expansion nozzle, is shown in Fig. 2. The computational fluid dynamics domain consists of an unstructured 3D grid with 121289 nodes and 566669 tetrahedral elements.

3.2 Process Modeling and Boundary Conditions

As was mentioned before, the model consists of two major sections: combustion chamber and expansion nozzle. The major interest was the analysis of the turbulent premixed combustion of propane and the evaporation of ethanol followed by its nonpremixed combustion that occurs in the torch (combustion chamber and expansion nozzle).

The combustion process model for turbulent reacting flows was implemented into ANSYS-CFX.11 as described above. The set of equations describing the physicochemical process were discretized and solved numerically by the finite volume technique. In addition, the mass flow rates of oxygen, propane, and the suspension (ethanol and nanoparticles) were defined at the inlets. In this process, the premixed flame is a lean-burn combustion (fuel equivalence ration <1), leaving excess oxygen in the system. For the premixed propane/oxygen combustion (chemical reaction model), the eddy dissipation model was applied (Ref 12-14), which assumes that the reaction rate is limited by the turbulent mixing rate.

Ethanol is injected into the combustion chamber as dispersed liquid particles (droplets), and the nanoparticles are injected at the same inlet to the combustion chamber as dispersed solids. It was assumed that during atomization, an initial uniform droplet diameter of 0.3 mm is generated (diameter of the injection nozzle), and that the suspension contains discrete nanosized titania material in the range of 100 nm to 10 μm in diameter. The initial conditions (mass flow, temperature, and pressure) at the inlets of the combustion chamber as well as the boundary conditions at the wall (combustion chamber and expansion nozzle) and at the outlet (nozzle) for this study are listed in Table 2.

The torch cooling is given as a water flow with water temperature $T = 10$ °C and velocity $v = 5.97$ m/s in a

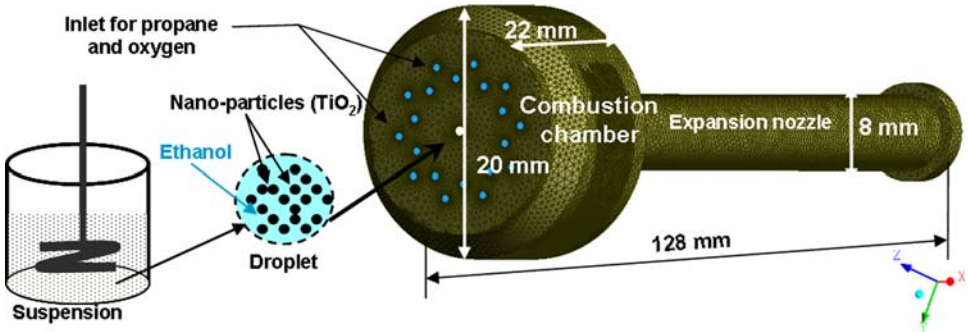

Fig. 2 Three-dimensional computational domain of the HVOF and HVSFS torch with injection positions of suspension and fuel gas/oxygen mixture

Table 2 HVOF and HVSFS initial and boundary conditions, using an oxy/fuel ratio of 0.9

Model parameters	Inlet $C_3H_8 + O_2$	Inlet C_2H_6O liquid	Inlet TiO_2	Wall	Outlet
Mass flow, kg s^{-1}	0.189×10^{-3}	0.917×10^{-3}	0.214×10^{-3}	...	...
Temperature, K	300	300	300	283.15	298
Pressure, Pa	...	...	...	...	1.05×10^3

channel ($l_{cha.} = 0.001$ m) along the torch wall (outside of the combustion chamber and the expansion nozzle). The Reynolds number (see Eq 4) of the water flow can be calculated as Re = 9140, which means that Re > 2300 corresponding to turbulent pipe flow. In this case, the Prandtl number (see Eq 6) is 0.742, and the Nusselt number is calculated to $Nu = 84.157$ using the Prandtl-Taylor analogy (see Eq 34). Finally, the heat transfer coefficient to be used as boundary condition for heat transfer through the torch wall by the water cooling can be estimated as $Q_{wall} = 24489.7$ W m^{-2} K^{-1}.

The governing mass, momentum, and energy balance equations (Eqs 21-24), together with the ideal gas law, were solved at high resolution scheme to achieve a convergent solution and to generate the boundary layer inside the torch wall. Due to high Reynolds numbers and large pressure gradients in the combustion chamber and in the nozzle, the κε-turbulence model was applied with the scalable turbulent wall function in order to implement wall friction and heat transfer into the model.

Particle breakup is modeled using the Blob method (Ref 16, 18) for disperse droplets and the ETAP method (Ref 18) for disperse solids, taking into account the Weber (Eq 7) and Reynolds number (Eq 5) of each particle. In the Blob method, it is assumed that a detailed description of the atomization and breakup processes within the primary breakup zone of the spray is not required. Spherical droplets with uniform size, $d_p = d_{nozzle}$, are injected which are subject to aerodynamically induced secondary breakup. The spray angle is either known or it can be determined from empirical correlations.

Modeling of the secondary, nonpremixed combustion of the vaporized ethanol solution associated with a premixed combustion system is a challenging task. The main difficulty is the ethanol phase change from liquid to gaseous, which must be modeled in a first step as ethanol mass transfer from dispersed liquid droplets to continuous gas. This is the precondition for combustion modeling with a diffusion flame model. Evaporation of the ethanol droplets is modeled using the liquid evaporation model described in Section 2.3. This model describes two-way coupling for heat and mass transfer between fuel/oxygen reaction flame (continuous gas) and particles (suspension) for the assumption that the continuous gas phase is at a higher temperature than the particles. The user-supplied coefficients for modeling of the ethanol saturation vapor pressure using the Antoine equation (see Eq 17) were estimated as $A = 7.506$, $B = 1739.914$, and $C = 238.131$ by experimental investigations (Ref 19). The boiling point of ethanol is at about 351.6 K at 1,000 Pa, while the temperature in the HVSFS combustion chamber is in the range of 3,600 K. Therefore, the heat transfer from the continuous gas to the ethanol droplet is determined by the convective heat transfer given in Eq 31.

For modeling of the chemical reactions after ethanol evaporation, the finite rate chemistry model (Ref 16, 17) is used to solve the rate of progress of elementary reactions taking place during diffusion combustion (nonpremixed ethanol vapor).

4. Simulation Results and Discussion

4.1 Simulation of Chemical Reacting Flow, Flame, and Suspension Properties

An overview of kinetic modeling for all common hydrocarbon combustion processes given by Westbrook and Dryer (Ref 17) contains chain-branching steps that produce CO and H_2 as primary products of hydrocarbon oxidation reactions on one side, and on the other side, contain the oxy-hydrogen (H_2O) reaction mechanism and CO oxidation (CO_2) in subsequent, slow secondary reaction processes.

For the simulation of HVOF and HVSFS fuel gas and ethanol suspension reaction with oxygen, results for the mass fractions of each species taking part in the combustion of premixed propane fuel with an excess of oxygen are shown in Fig. 3. Thereby, oxygen remnants can be observed in the torch after the complete consumption of C_3H_8 species. This excess oxygen reacts with ethanol C_2H_6O as diffusion flame (nonpremixed combustion of ethanol vapor) after ethanol evaporation (Fig. 3a).

In the results given in Fig. 3, the spray breakup of ethanol droplets in the combustion chamber can be observed. The mass fraction of C_2H_8O gas is close to zero after injection and increases rapidly after reaching the ethanol's boiling point at an axial position of approximately 0.022 m (at the outlet of the combustion chamber into the nozzle), where ethanol begins to evaporate until complete evaporation and phase change (liquid to gas). The point of total evaporation of ethanol, see Fig. 3(b) and (c), also locates the highest value of the ethanol gas mass fraction (mf ≈ 0.35) in the process. Downstream, gaseous ethanol is burned and the mass fraction decreases along the centerline.

It is noticeable that evaporation of ethanol mainly occurs in the area behind the nozzle entrance. This is due to the high-speed suspension injection in combination with the heat transfer from the flame to the cold particles (300 K at the entrance).

The heat and momentum transfer from the gas to the suspension particles strongly depends on the temperature and velocity difference between each phase. At high

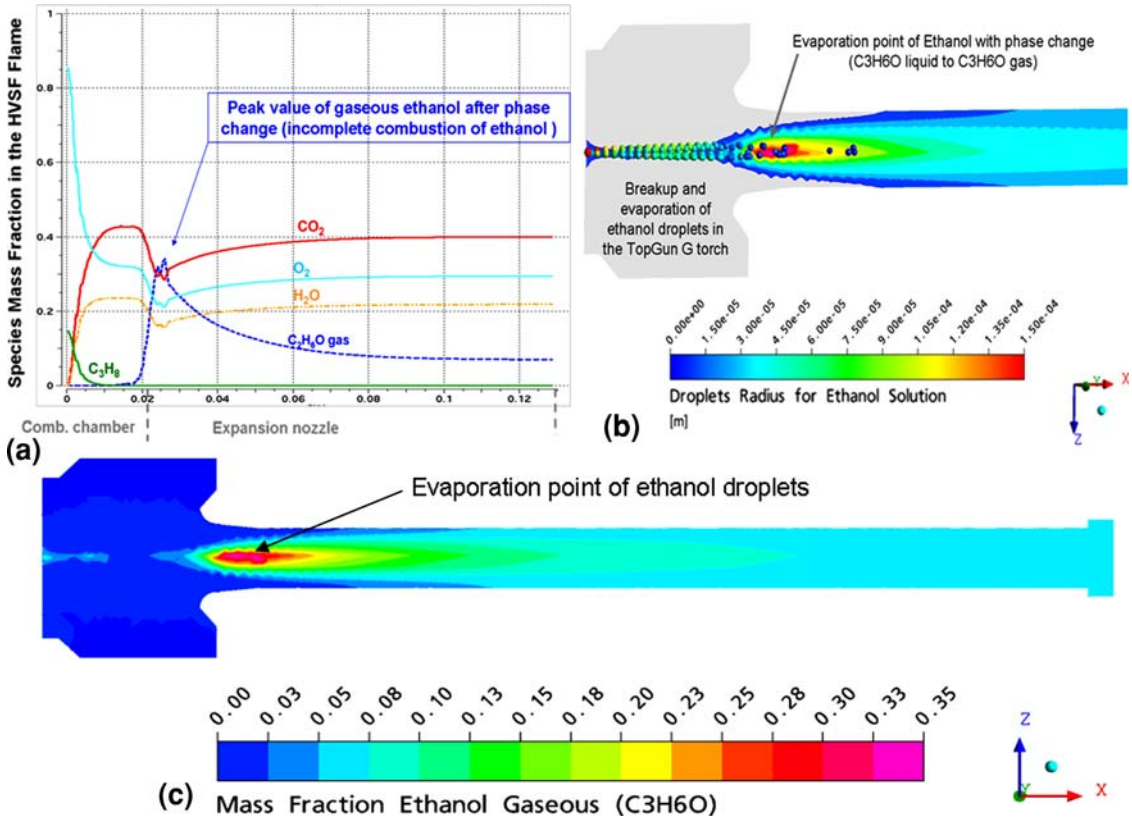

Fig. 3 Mass fraction profiles of each species derived from propane oxidation and ethanol evaporation (a), breakup and evaporation of ethanol droplets (b), and mass fraction contour of gaseous ethanol in the TopGun®-G torch (c)

relative velocities, the drag force on the particles (see Eq 27) is not only a function of the Reynolds number, but also a function of the Mach number. Furthermore, the heat transfer coefficient between gas and particles also depends on compressibility effects under these conditions.

In the combustion chamber, the gas temperatures increase due to premixed combustion to values above 3700 K and a pressure in the region 4×10^5 Pa (approximately 3.65×10^5 Pa at the centerline). Figure 4(a) shows the temperatures profiles of the continuous gas and the disperse particles (ethanol liquid until vaporization and titania particles with different size range.

The centerline profile of the continuous gas phase clearly shows the cooling effect due to ethanol vaporization taking place at the exit of the combustion chamber, which leads to a temperature loss of 700 K in the calculation as shown in Fig. 4(a). However, due to ethanol combustion, the reaction gases quickly increase in temperature up to the maximum values of approximately 3600 K along the centerline at the outlet of the torch.

The static pressure in the internal and external flow fields decreases and the gas velocity increases continuously, see Fig. 5, as the exhaust gases expand through the nozzle that has a convergent profile close to the combustion chamber and a straight profile close to the outlet. At the entrance to the nozzle, the Mach number increases. The gas is accelerated during expansion in the nozzle and reaches supersonic velocity (Mach number of 2.3) at the nozzle outlet.

The specific heat, density, and melting point of the particles are important properties to be considered for the choice of the appropriate fuel gas. In this study, titania powder was applied with a specific mass of 4230 kg/m^3, a specific heat capacity of 3.78 kJ/(kg K), a thermal conductivity of 10.4 W/(m K), and a melting point of approximately 2100 K.

4.2 Modification of the TopGun®-G Combustion Chamber

The maximum velocity of the combustion gas was calculated as approximately 1552 m/s close to the nozzle exit. However, due to their mass inertia, the solid particles do not follow the high gas acceleration in the combustion chamber, but are more or less separated from the gas depending on their size. Thereby, large particles are more inert than small particles. This leads to higher instabilities for smaller particles in the combustion chamber as show in Fig. 6(left).

The simulation results of the reaction mechanism and the flow transport properties show important particle instabilities in the combustion chamber. This is due to the high turbulence flow characterized by continuous fluctuations of the velocity which lead to fluctuations in scalars

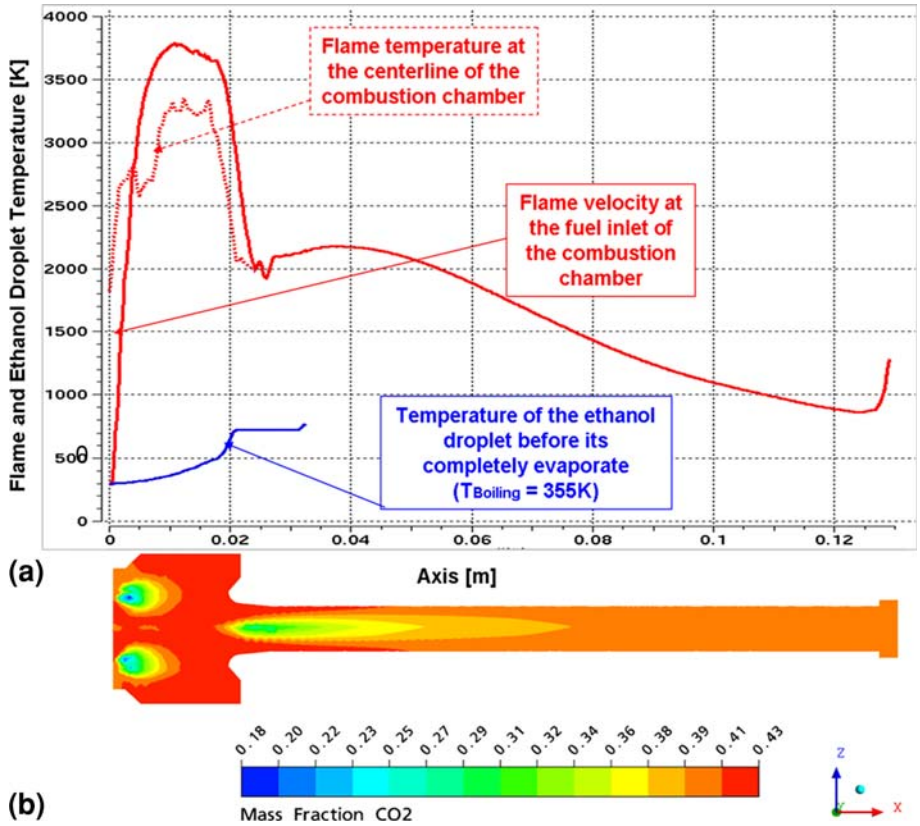

Fig. 4 Temperature profiles of HVSFS flame and ethanol solution (a) and mass fraction contour of CO_2 in the TopGun®-G torch (b)

mixture component (ethanol and oxygen) as shown in Fig. 6. These fluctuations in the flow velocity and the mixture component are a consequence of vortices generated by shear within the flow. The vortex motion shown in Fig. 6(right) greatly accelerates the mixing process between propane and oxygen. However, this effect also involves several instabilities of submicron-, and nano-scale particles due to their small mass inertias. Experimental studies of the HVSFS process show an important amount of particle deposition inside the combustion chamber, which is a harmful effect for process stability and equipment maintenance.

In order to avoid particle deposition in the combustion chamber and nozzle, optimizations experiments were made with the aim of reduced particle deposition due to improved flow behavior. The principal modification that was applied for flow optimization is the combustion chamber geometry. Therefore, the straight geometry was changed to a conical shape (see Fig. 6 and 7 for comparison).

Modification of the combustion chamber geometry led to good results regarding the micron- and nano-scale particles' trajectories in the combustion chamber. The single particles showed reduced wall contact in simulation experiments and the flow field showed a higher gas velocity at the wall of the combustion chamber, see Fig. 7. Experimental evaluation experiments with such a modified TopGun®-G torch geometry resulted in lower material deposition inside the torch.

5. Summary and Conclusions

High-velocity suspension flame spraying is a novel technology for direct processing of submicron- and nano-scaled particles to achieve dense surface layers in supersonic mode with a refined structure, from which superior mechanical and physical properties are expected. The application of solutions as a carrier fluid for nanoparticles in thermal spray systems is a new approach that features some thermophysical and thermochemical changes of HVSFS compared to the conventional HVOF process.

Three-dimensional modeling and analysis of the combustion and gas dynamic phenomena of the three-phase HVSFS process based on a numerical model for a conventional HVOF process was performed in this work for an industrial TopGun®-G torch, including modeling of ethanol evaporation followed by nonpremixed combustion of gaseous ethanol with excess oxygen from the fuel gas (propane)/oxygen combustion, and analysis of the interaction mechanisms between gas and liquid as well as between gas and particles. The thermal and flow fields of the reaction gas were solved by an Eulerian approach,

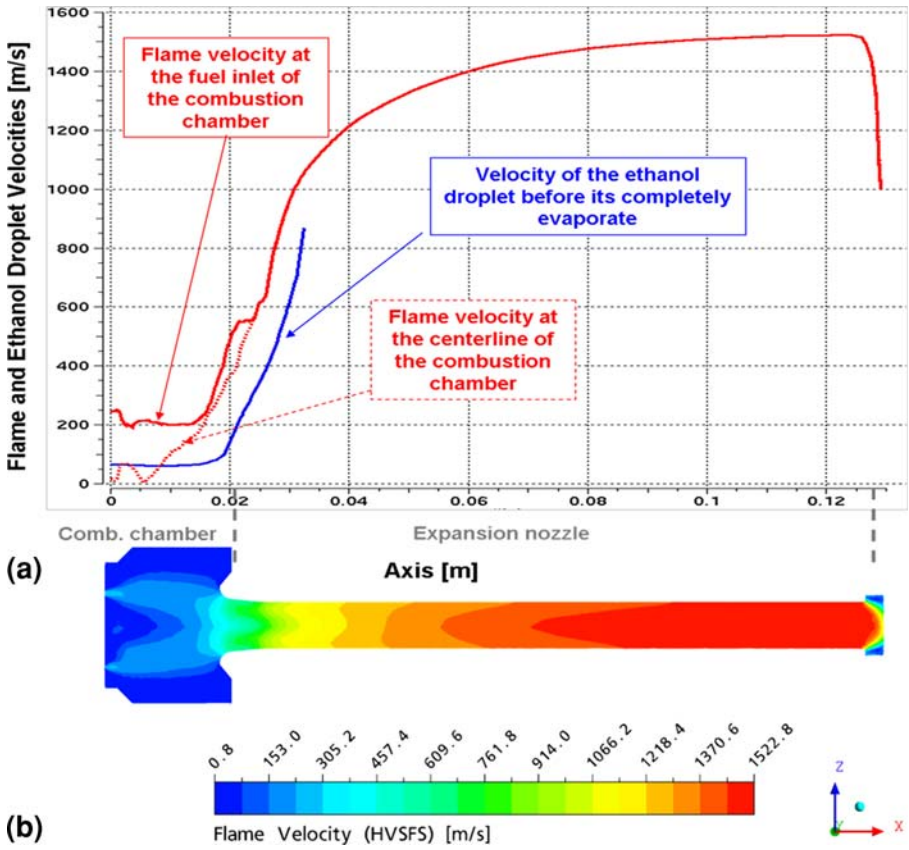

Fig. 5 Velocity profiles of HVSFS flame and ethanol solution (a) and velocity contour of HVSFS flame in the TopGun®-G torch (b)

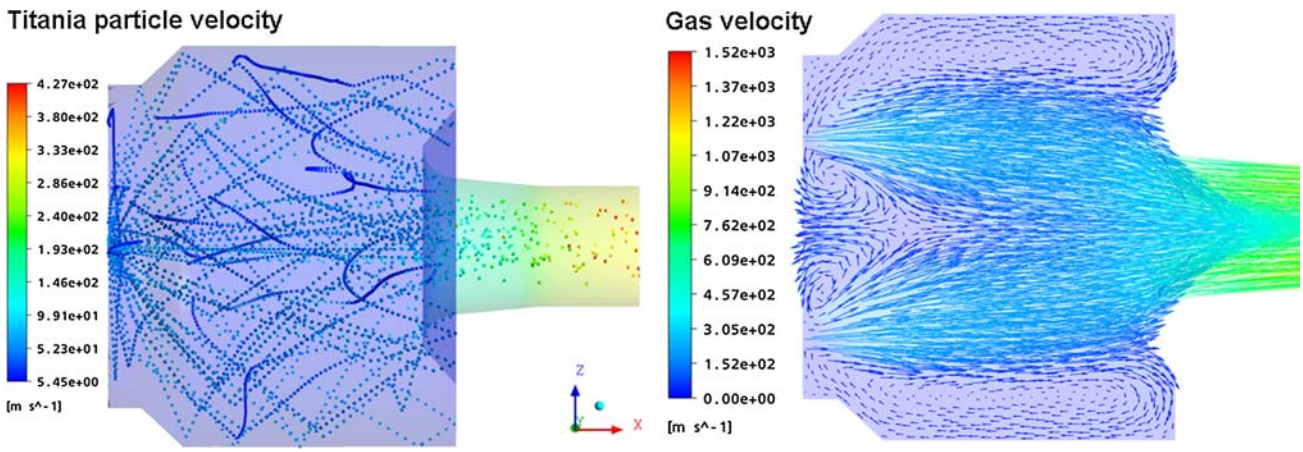

Fig. 6 Velocity and trajectories of TiO_2 particles (*left*) and velocity vectors of HVSFS flame (*right*) in the combustion chamber

whereas the particle in-flight behavior was simulated by a Lagrangian approach using the commercial CFD software ANSYS-CFX.11.

An Antoine equation assumption was utilized in the liquid evaporation model for determining the liquid droplet properties (temperature, velocity, diameter, etc.) during the energy transfer in the combustion chamber. Particle breakup is modeled using the Blob method for disperse droplets and the ETAP method for disperse solids, taking into account the Weber and Reynolds numbers for each particle. A uniform diameter assumption was used for the ethanol droplets, and a discrete diameter distribution was applied for the particle size of the solid particles (Titania powder in micron- and nano-scale). Two-way coupling was used for the energy and mass transfer between gas and liquid, while one-way coupling

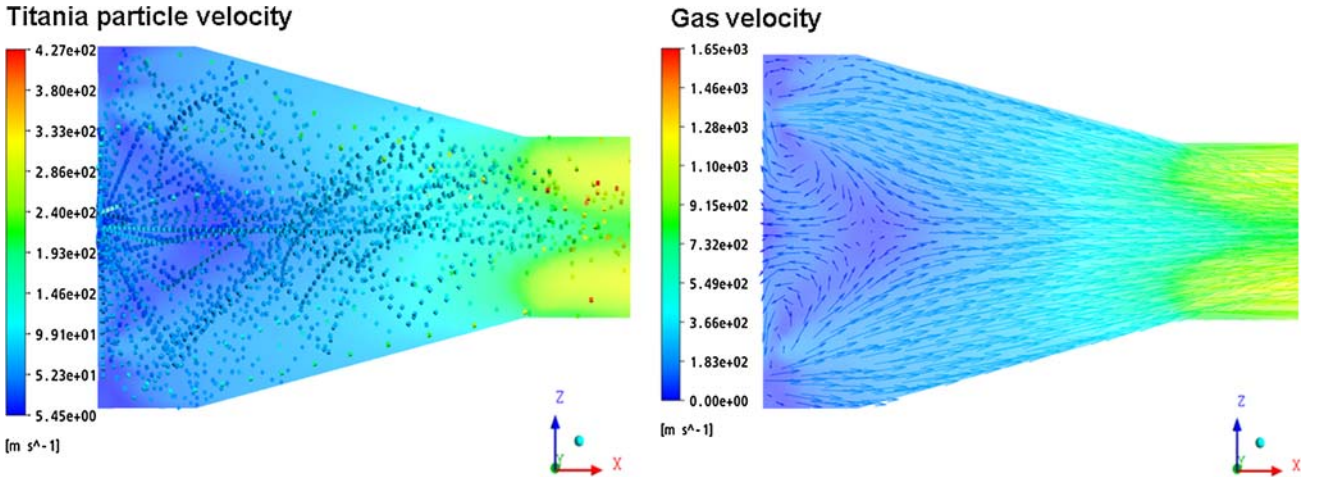

Fig. 7 Velocity and trajectories of TiO_2 particles (*left*) and velocity vectors of HVSFS flame (*right*) in the modified TopGun®-G combustion chamber

was used for the thermal and kinetic energy transfer from gas to solid particles, assuming that the particles have no distinct influence on the gas properties.

The aim of this work was the development of an analytical methodology for the analysis of the HVSFS thermal spray process toward improved process understanding and parameter optimization for specific applications. First results with propane as fuel gas, a fuel/oxygen ratio of 0.9, and ethanol as suspension medium show the distribution of chemical reaction species in the combustion chamber and expansion nozzle as well as the temperature and velocity fields of the gas flow. The evolution of the mass fractions of propane, ethanol, oxygen, and the exhaust gases along the torch centerline shows a clear correlation with the temperature of the gases, and thus, the temperature of the spray particles. Ethanol evaporates no earlier than inside the expansion nozzle due to the injection conditions, but also the increase in pressure in the combustion chamber due to ethanol evaporation, leading to later evaporation. Ethanol evaporation leads to a rapid decrease in flame temperature which is not compensated by gaseous ethanol combustion. At the same time, oxygen is not completely consumed by the ethanol combustion. The reason for this is that the reaction kinetics is controlled by the diffusion process (nonpremixed combustion) under the boundary condition of a high gas velocity. This also means that the gas temperature in the nozzle cannot be influenced by the oxygen content in the premixed oxy/fuel mixture. As a consequence, the spray particles, which are heated only after release from the suspension droplets, are heated at lower gas temperature and with lower dwell time compared to the HVOF process. The only possibility to change the heating characteristics of the spray particles is to move the position of ethanol evaporation inside the combustion chamber, and the most promising possibility for that (by keeping the injection boundary conditions, and thus, gas velocities constant) would be modification of the combustion chamber (mainly adaptation of its length).

Simulation results from previous Studies (Ref 12, 14) are be used to verified the HVOF-Flame properties calculated in this study.

Furthermore, simulation results have been successfully applied for improving the design of HVSFS torches in terms of particle deposition at the internal wall of the combustion chamber. Material deposition was mainly due to vortices at the boundary regions of the combustion chamber, including low velocity areas, which were verified by simulation experiments. A modified, divergent design of the combustion chamber was developed by analysis of different geometries with the models described in this work, leading to a more homogeneous flow velocity inside the combustion chamber. Experimental verification of that torch design showed a decrease of material deposition as predicted by simulation results.

Further work on this subject will include an optimization process of the HVSFS thermal spray system, aiming for an accurate and detailed description of the flow field in the free jet range between the torch outlet and the substrate, which was not considered in the present study. Furthermore, advanced studies on the instabilities of the particles' flow paths in the HVSFS combustion chamber have to be accomplished.

References

1. L. Pawlowski, *The Science and Engineering of Thermal Spray Coatings*, 2nd ed., Wiley, Chichester, 2008
2. J.R. Davis, *Handbook of Thermal Spray Technology*, ASM International, Materials Park, OH, 2004
3. G. Kreysa and M. Schütze, *Corrosion Handbook*, Wiley-VCH, New York, 2006
4. C.C. Koch, *Nanostructured Materials: Processing, Properties and Potential Applications*, Noyes Publications, Norwich, NY, 2002
5. Y. Lu and P.K. Liaw, The Mechanical Properties of Nanostructured Materials, *J. Metal.*, 2001, **53**(3), p 31
6. R. Gadow, A. Killinger, and J. Rauch, New Results in High Velocity Suspension Flame Spraying (HVSFS), *Surf. Coat. Technol.*, 2008, **202**(18), p 4329-4336

7. H. Kassner, R. Siegert, D. Hathiramani, R. Vassen, and D. Stoever, Application of Suspension Plasma Spraying (SPS) for Manufacture of Ceramic Coatings, *J. Therm. Spray Technol.*, 2008, **17**, p 115-123
8. M. Gell, E.H. Jordan, M. Teicholz, B.M. Cetegen, and N. Padture, Thermal Barrier Coatings Made by the Solution Precursor Plasma Spray Process, *J. Therm. Spray Technol.*, 2008, **17**, p 124-135
9. P. Fauchais, R. Etchart-Salas, V. Rat, J.F. Coudert, N. Caron, and K. Wittmann-Ténèze, Parameters Controlling Liquid Plasma Spraying: Solutions, Sols, or Suspensions, *J. Therm. Spray Technol.*, 2008, **17**, p 31-59
10. G. Bolelli, J. Rauch, V. Cannillo, A. Killinger, L. Lusvarghi, and R. Gadow, Investigation of High-Velocity Suspension Flame Sprayed (HVSFS) Glass Coatings, *Mater. Lett.*, 2008, **62**, p 2772-2775
11. A. Killinger, M. Kuhn, and R. Gadow, High Velocity Suspension Flame Spraying (HVSFS), a New Approach for Spraying Nanoparticles with Hypersonic Speed, *Surf. Coat. Technol.*, 2006, **201**, p 1922-1929
12. E. Dongmo, M. Wenzelburger, and R. Gadow, Analysis and Optimization of the HVOF Process by Combined Experimental and Numerical Approaches, *Surf. Coat. Technol.*, 2008, **202**, p 4470-4478
13. L. Mingheng and P.D. Christofides, Multi-Scale Modeling and Analysis of an HVOF Thermal Spray Process, *Chem. Eng. Sci.*, 2005, **60**, p 3649-3669
14. E. Dongmo, A. Killinger, M. Wenzelburger, and R. Gadow, Numerical Approach and Optimization of the Combustion and Gas Dynamics in High Velocity Suspension Flame Spraying (HVSFS), *Surf. Coat. Technol.*, 2008, **202**(18), p 4329-4336
15. R. Etchart-Salas, V. Rat, J.F. Coudert, and P. Fauchais, Influence of Plasma Instabilities in Ceramic Suspension Plasma Spraying, *Proc. ITSC 2007, Thermal Spray 2007: Global Coating Solutions*, ASM International, 2007, p 621-626
16. K.K. Kuo, *Principles of Combustion*, 2nd ed., Wiley, Hoboken, NY, 2005
17. C.K. Westbrook and F.L. Dryer, Chemical Kinetic Modeling of Hydrocarbon Combustion, *Prog. Energy Combust. Sci.*, 1984, **10**, p 1-57
18. S. Prakash and W.A. Sirigano, Theory of Convective Droplet Vaporisation with Unsteady Heat Transfer in the Circulating Liquid Phase, *Int. J. Heat Mass Trans.*, 1980, **23**, p 253-268
19. www.ddbst.com, http://ddbonline.ddbst.de/AntoineCalculation/AntoineCalculationCGI.exe